

# Image Cover Sheet

**CLASSIFICATION**

UNCLASSIFIED

**SYSTEM NUMBER**

511902



**TITLE**

Critical Strain Energy Density from Tensile Specimens

**System Number:**

**Patron Number:**

**Requester:**

**Notes:** Paper #28 contained in Parent sysnum #511874

**DSIS Use only:**

**Deliver to:** CL



# Critical Strain Energy Density from Tensile Specimens

by G.R. Pelletier and J.R. Matthews

Defence Research Establishment Atlantic  
P.O. Box 1012, Dartmouth, Nova Scotia, B2Y 3Z7

## ABSTRACT

Fracture has always been a serious concern in the design and repair of steel structures such as ships. Because of these concerns, much research has been ongoing in the causes of fractures and in ways which they could be predicted and thus prevented.

The objective of this study was to find, test and evaluate a method for measuring the critical strain energy density with tensile specimens.

Plastic strain at fracture (real strain) was measured for gauge lengths of 1.25 mm and 1.125 cm using an etched grid. Real stress, the force divided by the reduced area, was also measured. Complexities in these two measurements were dealt with by detailed numerical analysis resulting in approximate average real stress - real strain curves that, in the transition zone, displayed decreasing strain energy density with temperature.

## 1.0 Introduction

Fractures in ships, buildings and bridges have always been a serious concern. Especially, in the areas of design and repair. Because of this, much research has been ongoing in the causes of fractures and in ways which they could be predicted and thus prevented.

This report will concentrate on techniques by which fractures can be predicted and thus prevented. The objective of this study was to find, test and evaluate a method for measuring the critical strain energy density with tensile specimens.

There are an alarming amount of failures occurring in ships, bridges and buildings. These failures have motivated extensive investigations in various countries. It was observed in the early 1940's that fractures were occurring more frequently at low temperatures. Many fractures occurred suddenly, without warning, at low nominal stresses. Investigations into these fractures revealed that the steels experienced states of extreme brittleness.

It was slowly recognized that there existed service temperatures where the structures were susceptible to brittle fractures even though the material was thought to be ductile. Included in this report are discussions of some of these failures and the result of their respective inquiries.

Tensile tests were performed to obtain data so that the strain to fracture (plastic and total), and the critical strain energy density could be evaluated in the transition zone.

## 2.0 Background

The background section discusses the various investigations that occurred as a consequence of certain steel failures. Presented herein are some of the conclusions and recommendations from the formal inquiries that took place as a result of the failures.

### 2.1 Boston Molasses Tank

One of the most famous tank failures was that of the Boston molasses tank, which failed in January 1919. The tank contained 2,300,000 gallons of molasses when it failed. Twelve people were drowned, 40 were injured and several horses were drowned. Houses were damaged, and a portion of the Boston Elevated Railway structure was knocked over.

An extensive lawsuit followed, and many well-known engineers and scientist were called to testify. After years of testimony, the court appointed auditor handed down the decision that the tanks failed by over-stress. When the auditor was asked to comment on the conflicting technical testimony, he was quoted as saying "amid this swirl of polemical scientific waters...[he] at times felt that the only rock to which he could safely cling was the obvious fact that at least one half of the scientists must be wrong" [1]. His comment summarized the state of knowledge among engineers regarding brittle fractures. At times, it seems that the statement is still true today.

### 2.2 Liberty Class & T-2 Tankers

Over twenty-five hundred Liberty Class Ships were produced between 1941 and 1945 for the Second World War [2]. The mass produced Liberty Ships were the first all-welded ships. These cargo ships were designed for a service life of five years, and took

less than 60 days to construct [3]. One yard actually built a Liberty ship in four days, 15 hours and 30 minutes [4]. Figure 1a is a photograph of a Liberty Ship.

Welding provided savings in time, manpower and training [5]. Without welding, it would have been impossible to build, at such speeds, the enormous merchant fleet of Liberty Class Ships.



**Figure 1a. Liberty Ship.**

Many of the Liberty Ships failed. Over a thousand ships suffered from cracks in varying degree, 190 ships sustained serious fractures, and twelve ships broke in two [6]. Design errors and inferior workmanship were shown to be factors in these failures [7]. However, the Liberty ships were made from steel that had low toughness [8]. Shown in Figure 1b are Charpy transition curves for the Liberty ship, SS Simon Willard, the SS Warrior, and the average results from 26 Liberty ships.

The SS Simon Willard was one of the worst case scenarios. The midpoint Charpy transition temperature for the Liberty ships was found to be approximately  $32^{\circ}\text{C}$ , while the midpoint Charpy transition temperature for the SS Simon Willard was found to be approximately  $50^{\circ}\text{C}$ . The midpoint Charpy transition temperature for the SS Warrior was  $-5^{\circ}\text{C}$ . Many failures were initiated by fatigue cracks which nucleated at the corner of square hatches [2]. In the earlier riveted ships, the riveted plates acted as crack arresters, preventing catastrophic fractures from occurring, but the overall incidence when size was factored in, was no better.

The T-2 tanker SS Schenectady was the first all-welded tanker built by the Kaiser Company. She was launched in late 1942. While the Schenectady was afloat at dock in early 1943, she broke in two. Figure 2 is a photograph of the SS Schenectady.

The night of the failure the air temperature had fallen from  $3^{\circ}\text{C}$  to  $-5^{\circ}\text{C}$ . The ship broke in two, in a brittle manner, across the deck at a point abaft of midship. The ship jack-knifed, leaving a gap 10 feet wide in the deck. The vessel was ballasted as for the trial trip, the bending moment was about half the maximum designed bending moment [5].

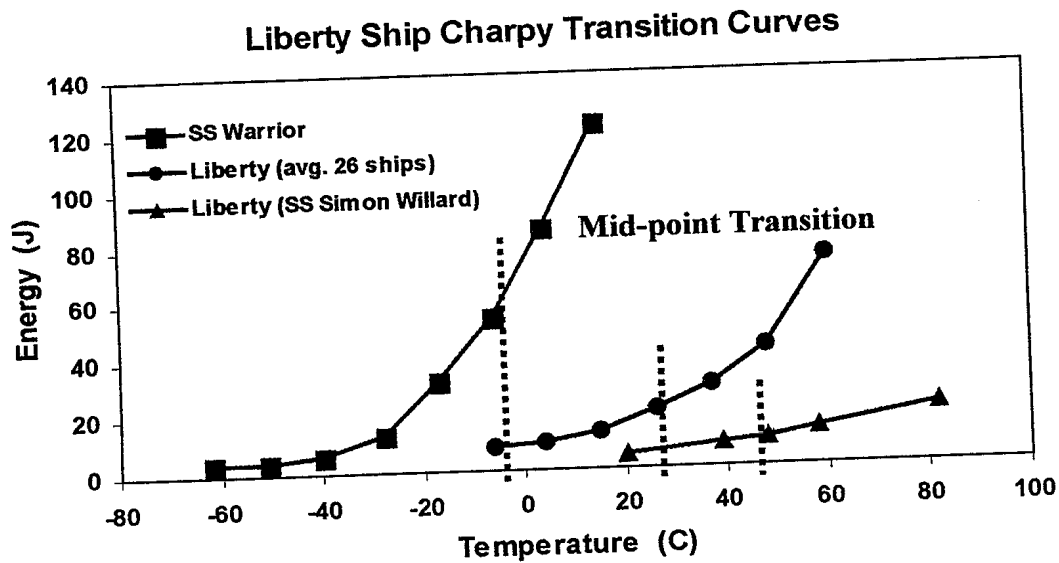


**Figure 1b. Liberty Ship Charpy V-Notch Transition Curves.**

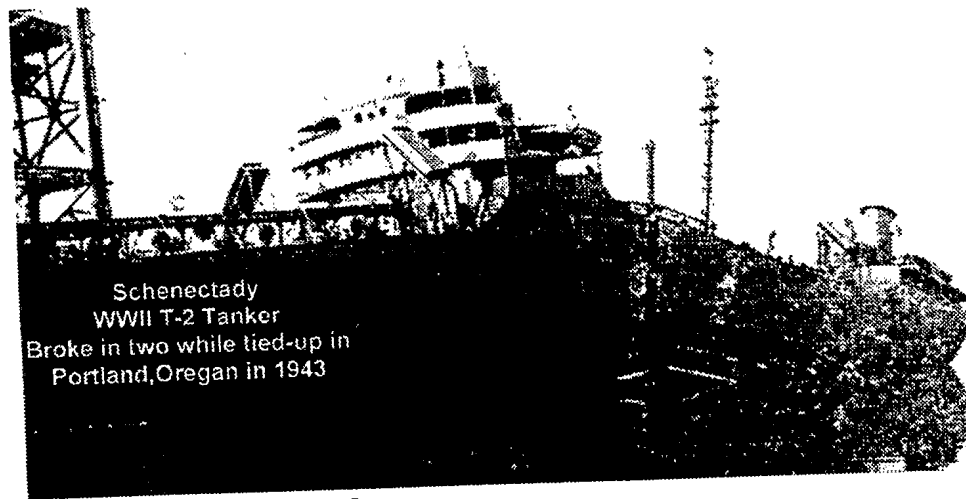


**Figure 2. SS Schenectady.**

The investigation into the failure found that there was a lack of uniformity in the quality of steel used for the hull. Low impact values at room temperature were obtained in impact tests, while complete brittleness occurred at  $-6^{\circ}\text{C}$ . There were no specifications in place at this time which required impact tests on the steel.

In 1943, the Admiralty Ship Welding Committee was formed in England [9]. The committee's prime directive was to investigate and find solutions to the failure problems occurring in welded ships. Ships were breaking in two for reasons other than war, collision, or stranding. The failure of the all-welded American tanker, the Schenectady, was a significant catalyst for the committee formation. The committee sponsored several

experiments. The objective of these experiments was to measure stresses and deflections in critical locations in both riveted and welded construction. Several features emerged from these experiments:

- Notches and sharp changes in sections should be avoided;
- There was a tendency for fractures to occur more frequently when the ship operated at low temperatures;
- Fractures in welded ships were occurring suddenly, they were sharp and accompanied by very little deformation or reduction in thickness at the fractured edges;
- Few fractures followed the weld. When the fracture started at a faulty weld, it proceeded into virgin plate;
- Most serious fractures in welded ships have been brittle. Notched tensile test samples taken from the vicinity of fractures have displayed the property of notch brittleness at temperatures within service range; and
- An increase in plate thickness tends to increase the possibility of a brittle type fracture.

It was concluded by the Committee that a remedy to the welded ship fracture problem was to eliminate the use of notch brittle steel in ship construction.

In 1946 the Secretary of the U.S. Navy assembled a Board of Inquiry into welded ship failures. Several relevant features emerged from this inquiry, they are as follows:

- All fractures investigated started at a discontinuity involving design or workmanship;
- Statistically, the age of the ship had no appreciable influence ;
- Steel from the fractured plates complied with the test requirements for ship steel (tensile strength);
- Fractures occurred more frequently at low temperatures;
- Killed steel is less susceptible to failure than semi-killed steel; and
- Metallurgical variables, such as grain size, deoxidization and plate thickness are important.

Sadly, the Admiralty Committee and the US Navy Inquiry, failed to appreciate the significance of their observations. This was perhaps due to the non-conservative nature of the Charpy test (structural transition is much worse than Charpy transition).

### 3.0 Fracture Control Theory

Material testing involves methods for systematic measuring and evaluation of the mechanical properties of materials. The properties measured in this report include strength and toughness.

The strength properties are related to the ability of a material to resist applied forces. Toughness measurements are related to the ability of a material to carry a load in the presence of a defect [10]. The toughness exhibited by steel is a weak function of the rate of loading and a strong function of temperature.

Steel structures that operate safely in warmer climates can suddenly fail in a brittle manner under colder conditions. This type of failure has been termed "brittle fracture". It was slowly recognized in the late 1940's that there existed service temperatures where the structure experienced brittle fracture even though the material was thought to be ductile. The antonym of a brittle fracture is a ductile fracture. Ductile fractures are characterized by their plastic deformation when a load is applied. The surface of a fractured ductile material has a fibrous texture with silky, dull-grey appearance, while the surface of a fractured brittle material has a bright granular appearance. The likelihood of a brittle fracture occurring increases as the temperature decreases. Thicker and wider sections and the presence of defects also reduce the capacity for plastic deformation to occur before fracture.

Brittle fractures have been, and still are one of the leading sources of steel casualties. Because of this, much time and effort has gone into the research of brittle fracture. Three conditions must be present for a brittle fracture to occur: i) stresses must be present; ii) there must be a crack forming flaw; and iii) structural transition must be lower shelf. The stresses may be present in the form of applied stresses, an example being wave action on a ship, or as residual stresses. Residual stresses are stresses that can not be measured non-destructively with the aid of strain gauges, these include hydrostatic stresses, welding residual stresses, fabrication restraint stresses, and thermal stresses. The crack forming flaw may be in the form of a welding defect such as lack of fusion, slag, porosity, fatigue cracking from applied cyclic strain, and geometric discontinuities.

Transition curves can be constructed from data obtained from Charpy V-Notch Impact ( $C_V$ ) and Dynamic Tear (DT) tests. The most effective way of predicting structural performance of a given material is through dynamic tear testing. The results obtained with DT specimens are much more meaningful than those obtained with the Charpy specimen. Past tests have shown that transition behaviour for a Charpy size specimen can be approximately 50°C to 100°C below the larger DT specimens [11]. Figure 3 is a schematic representation of the Charpy V-notch, the dynamic tear, and the estimated structural transition curves. In designing against brittle fractures it is of extreme importance that the minimum service temperature of the structure's steel must coincide with the upper shelf of the structural transition curve. It is therefore necessary to determine the structural transition of the steel and to design within the minimum service temperature of the surroundings and selected materials. From the structural transition curve it is possible to determine if the structure will exhibit ductile behaviour under all service conditions. Structures are subjected to a wide range of loading conditions and service temperatures. Service loading conditions can be significantly different for structures that are placed on land as compared to those that are located in water.



Structures immersed in seawater have a minimum service temperature of approximately  $-2.5^{\circ}\text{C}$ , while structures that are exposed to the air and wind may be subjected to service temperatures as low as  $-50^{\circ}\text{C}$  [6].

The Charpy V-Notch impact test has limitations. The small specimen used in the test lacks the constraint and the degree of triaxiality that exists in a larger structure. The Charpy test specimen is too small in size. Because of this small size it does not mimic the structure's behaviour. Therefore, the Charpy test requirements can not guarantee ductile behaviour. G. E. Dieter [12] outlined that the chief deficiency of the Charpy impact test is that the small specimen is not always a realistic model of the actual structure. At a particular service temperature the standard Charpy specimen shows high shelf energy, while the actual structure exhibits low toughness at the same temperatures.

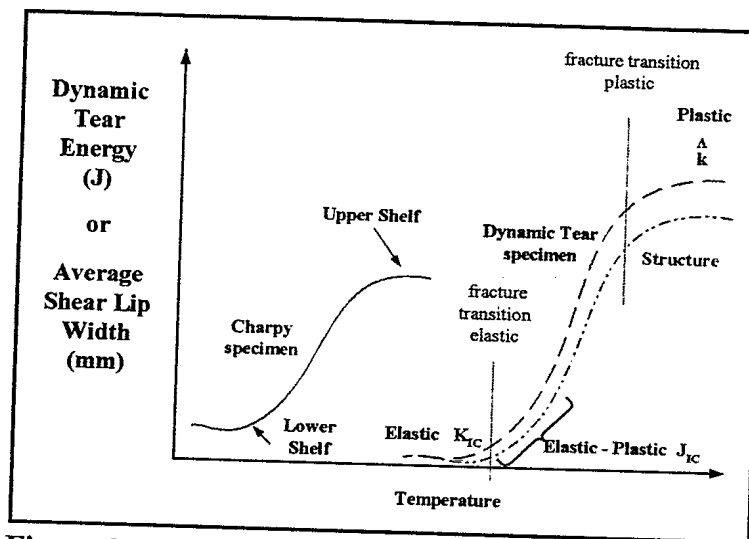


Figure 3. Transition Curves.

Transition curves can also be constructed from the shear lip width measurements obtained from the tested DT specimens. The shear lip information is equivalent to the energy information for characterizing the toughness of carbon and low alloy steels and their weldments [13]. Because the shear lip data is always available for re-examination and inexpensive to obtain, it is the preferred method for evaluating the transition behaviour of steels and weldments.

Analysis methods and formula also vary depending on the constraint and the degree of plasticity [10]. There exists different analysis for linear elastic fractures, elastic plastic fractures, transition fractures, and fully plastic fractures. Serious errors occur when the analysis of one level is applied to that of a different level. Errors can be avoided by staying within the bounds of the analysis listed in Table 1 and illustrated in Figure 4. There exists no accepted formula, nor method of analysis for the transition zone shown in Figure 4. The primary objective of this research report is to attempt to measure strain to fracture and critical strain energy density with the use of tensile specimens and to determine if these properties are relevant in transition.

Table 1. Constraints and Formulas.

Condition	Formula
Plane strain linear elastic	$a, b, B > 50r_y$ $a, b, B > 50/6\pi (K_{Ic}/\sigma_y)^2$
Plane stress linear elastic	$a, b > 50r_y$ $a, b > 50/2\pi (K_c/\sigma_y)^2$
elastic-plastic	$a, b, B > 50J/\sigma_y$
between elastic-plastic & fully plastic	$\epsilon_f \text{ or } (dW/dV)_c$
fully plastic	$k = \sigma_y/2$

Where  $a$  is the crack length;  $b$  is the length of the un-cracked ligament;  $B$  is the specimen thickness;  $K_{Ic}$  is the plane strain fracture toughness;  $J_{Ic}$  is the elastic plastic fracture toughness;  $k$  is the flow stress in shear;  $\epsilon_f$  is the fracture strain;  $(dW/dV)_c$  is the critical strain energy density;  $s$  is the shear lip width; and  $\sigma_y$  is the yield strength [10].

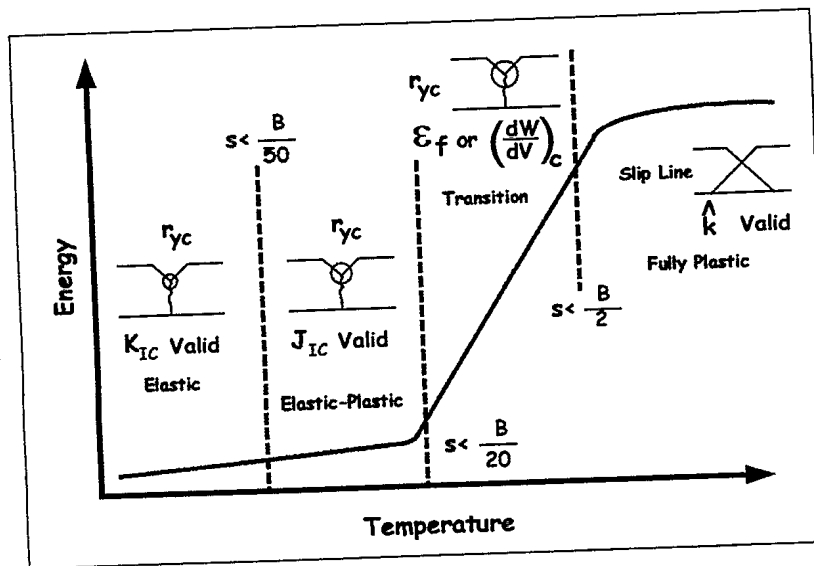


Figure 4. Transition Curve.

#### 4.0 Stress Strain Curve: Theory and Practice

Data obtained through tensile testing can be used to plot stress-strain curves. The engineering stress-strain curve is constructed by computing stress in terms of load divided by the original cross-sectional area, and the strain as the extension divided by the original gauge length over which the extension is measured. Figure 5 illustrates an engineering stress-strain curve. The elastic regime represents the area where a material will recover its original shape when a deforming load is removed. The elastic regime is a linear relationship where Hooke's law applies. A material in this region will relax to its initial form when the load is released. The yield stress represents a critical stress above which deformation will be permanent. Relaxing the load in this region will not allow the material to return to its initial form. The point marked "fracture" gives the fracture stress (fracture

load divided by the original cross-section). This is one of the real short comings of the engineering stress strain curve (force divided by the cross section at fracture is more significant).

The strain at fracture is represented by equation 1. The equation takes into account the original length and the length at fracture.

$$\epsilon_f = \frac{L_f - L_i}{L_i} \quad (1)$$

The strain necessary to deform the specimen from maximum load to fracture is called the necking strain, as necking usually begins at maximum load for most metals. The

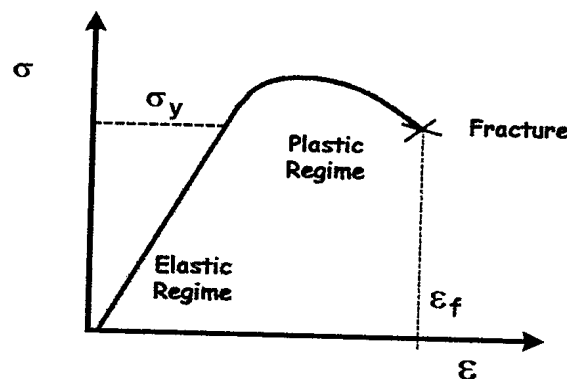


**Figure 5. Typical Engineering Stress-Strain Diagram.** (In this schematic the fracture stress is load divided by original cross-sectional area)

location of the maximum load on a stress-strain diagram is shown in Figure 6. After maximum load the specimen experiences an increase in stress. This increase is the result of a decrease in the cross sectional area of the specimen due to necking. Materials that show permanent necking before fracture do not have a uniform strain distribution along the length of the tensile specimen. The exact distribution of strain is a function of the metal, the gauge length, and the cross-sectional area of the specimen. Figure 8a illustrates that the area under the stress-strain curve will be lower for a less ductile material than a highly ductile material. The same is true of a material with less strain hardening, it will have a smaller area under the curve than a highly strain hardened material. The more strain hardened a material, the greater the amount of deformation away from the necking region. The shorter the gauge length, the greater the percentage elongation. Specimens that are to be compared must be geometrically similar. Therefore, the ratio of gage length to diameter must be a constant. The American convention is to have a tensile specimen with an L/D ratio of 4. The German standard calls for a L/D ratio of 10, while the British standard calls for a ratio of 3.54.

By increasing the thickness of a specimen, while maintaining a constant gauge length, the fracture elongation will increase until the length divided by the diameter reaches unity. Once unity has been obtained, the fracture elongation will decrease as the specimen thickness increases. This can be seen in Figure 8b. This data was obtained from research performed by the United States Naval Research Laboratory (NRL) in

Washington, DC [14]. NRL investigated the possibility of using tensile specimen size and geometry effects to accurately and uniquely assess the uniaxial continuum stress-strain curve. Reduction of tensile specimen load-displacement data to uniaxial continuum stress-strain data valid at large deformation is thought not to be possible for continuum material specimens which exhibit necking [14]. Valid uniaxial continuum stress-strain data is required for accurate finite element analysis, deformation prediction and design application. The necking phenomenon in specimens has been a difficult barrier to overcome so that accurate characteristics of a given material can be found. Focusing on real stress - real strain may be the answer.

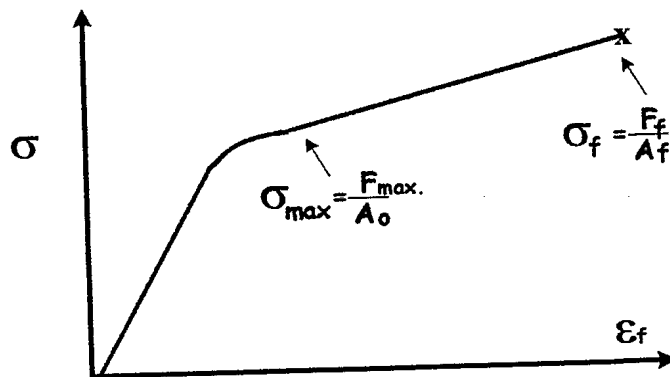


Figure 7. Real Stress - Real Strain Diagram.

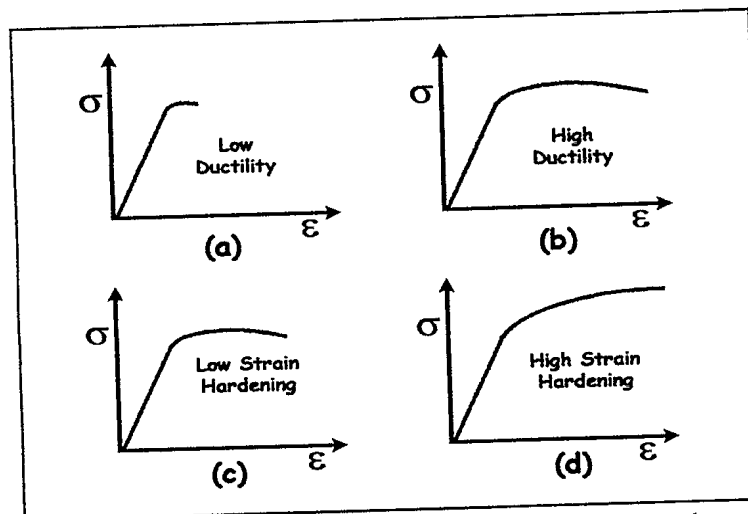


Figure 8a. Effect of Ductility and Strain Hardening on Engineering Stress-Strain Diagram.

The area under the stress-strain curve at fracture represents the critical strain energy density  $(dW/dV)_{critical}$ . This area is an indication of the amount of work per unit volume which can be done without failure occurring. The area under the stress-strain curve can also be referred to as the toughness of a material. The form of the stress-strain curves (engineering stress-strain versus real stress - real strain) is critical to succeed in determining  $(dW/dV)_{critical}$ .

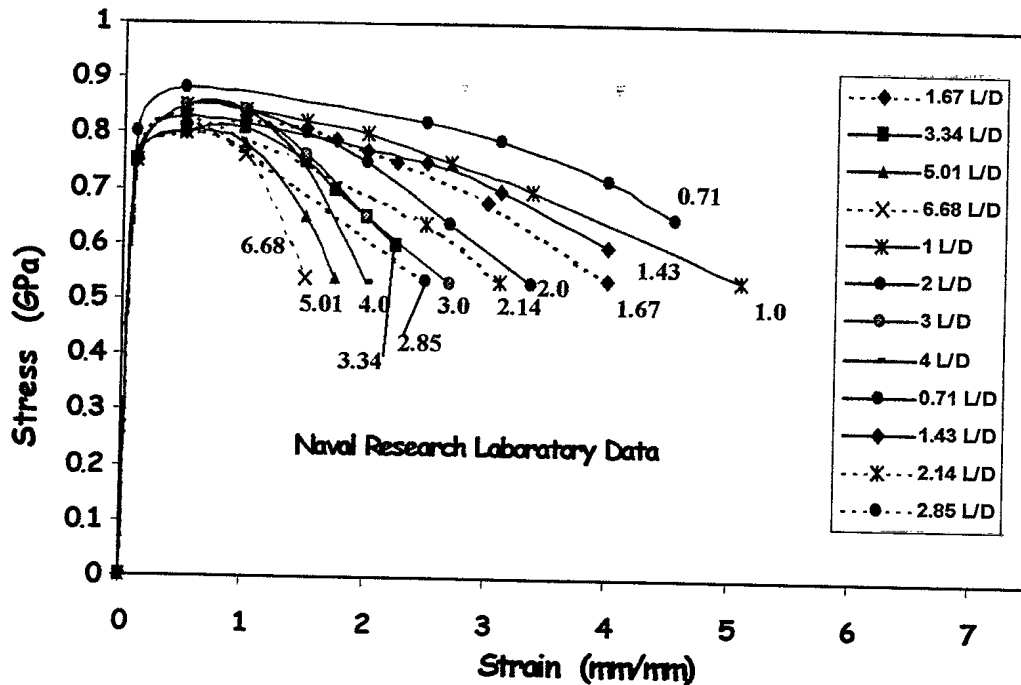


Figure 8b. Effects of Length/Diameter on Stress-Strain Diagram.

## 5.0 Material & Method

### 5.1 Materials

Structural quality steel plates used for general engineering purposes must comply with the requirements set forth by CSA Standard CAN3-G40.20-M, General Requirements for Rolled or Welded Structural Quality Steel. This Standard specifies specific requirements for analysis, number of tests, test preparation, methods of tests, permissible variations in dimensions and mass, repair, marking, inspection, re-tests, rejections, reports, packaging and loading.

The steel used in this research report was 350WT. The plate was a Fleet Maintenance facility (FMF) stores item. This item was stocked following the construction of the Canadian Patrol Frigates. The Stelco Steel Plant in Canada certified that the Canadian plate was made of Can/CSA-G40.21-M92 GRD 350 WT Category 5 steel. The "WT" indicates that the steel is weldable and has a toughness requirement. Steels of this type are required to meet specific strength and Charpy V-Notch impact requirements and are suitable for welded construction where notch toughness at low temperature is a design requirement.

Outlined in Table 3 are the chemical compositions set forth by the Standard. According to the Standard, materials that differ from the requirements of Table 3 (except for carbon, manganese, phosphorus, and sulphur contents) may be considered as meeting the requirements of the Standard, provided that all of the specified mechanical properties have been obtained. Included in the table are two independent analyzes which were done on portable analytical instruments.

**Table 3. Chemical Composition of 350WT Steel.**

	C	Mn <sup>1</sup>	P	S	Si	Cr	Ni	Cu
<b>Standard</b>	0.22 max.	0.80-1.50	0.03 max.	0.04 max.	0.15-0.40			
<b>Spectro Port</b>	0.054	1.17	0.018	0.012	0.210	0.029	<0.005	0.010
<b>Metallurgist XR</b>	na	1.45	na	na	na	0.21		

	Al	Co	Nb	Ti	V <sup>2</sup>	W	Pb	Mo	Fe
<b>Standard</b>					0.10 max. <sup>3</sup>				98.70 max.
<b>Spectro Port</b>	0.049	0.150	0.022	0.024	0.069	0.004	<0.0009	<0.010	98.2
<b>Metallurgist XR</b>	na		0.03		0.07				97.93

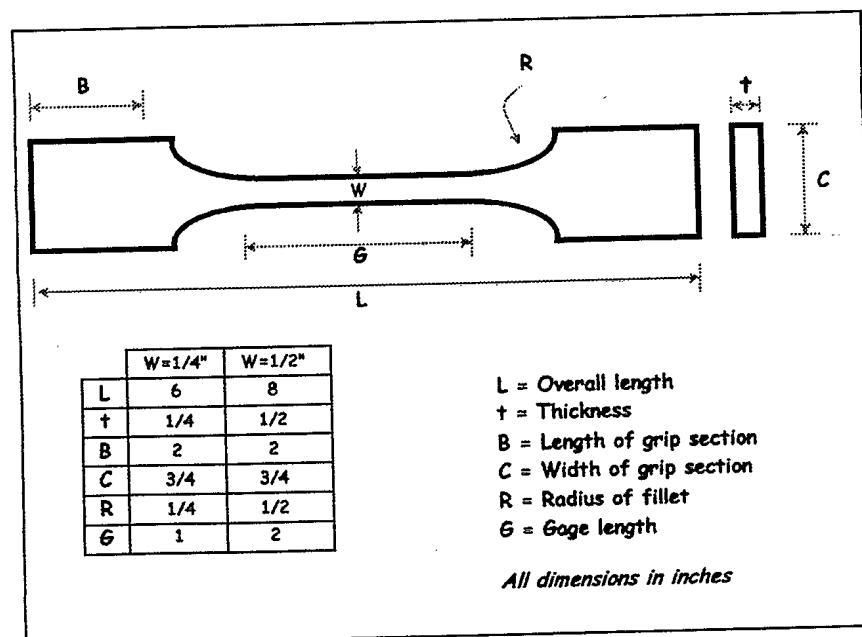
1. The manganese content may be increased provided the sum of the carbon content plus 1/6 of the manganese content does not exceed 0.40% for Grade 350WT.

2. Aluminum may be used as a grain refining element, however it shall not be included in the summation of grain refining elements. The elements columbium and vanadium may be used singly or in combination up to the total percentage indicated.

3. A nitrogen content of 0.01-0.02% may be used if the nitrogen content does not exceed 1/4 of the vanadium content.

### 5.1.1 Tensile Specimens

Twelve tensile specimens were machined from the 350WT plate. The specimen dimensions are shown in Figure 9. The specimens were machined in accordance to ASTM Standard E8. Six specimens were cut with a width (W) of 1/4 inch, and six specimens were cut with a width of 1/2 inch. The specimens were cut in the L-T direction (length parallel to rolling direction). The specimens were marked with an electro-etch grid of 1.25 mm.

**Figure 9. Schematic of Tensile Specimen.**

## 6.0 Testing

Tension tests were performed on an Instron interfaced with "daqware" software. Figures 10a & b are photographs of the apparatus. The specimens were fractured inside an enclosed compartment so that the temperature could be controlled. The specimens were cooled with CO<sub>2</sub> gas. Specimens with two different gauge lengths (1 & 2 inch) were tested at five different temperatures (-40 to 10°C). Three different parameters were recorded during testing: strain, stroke, and load. The computer was set for analog input, at a maximum (100%) of 10 volts. This related 10 volts to 22000 lb. load, 2-inch stroke, ½-inch strain. The strain was recorded with the use of an extensometer gauge. One hundred data points were recorded per second. Conversion of the data was necessary from volts to pounds and inches.



Figure 10a. Tensile Test Set-up.



Figure 10b. Grips with Specimen & Extensometer.

## 7.0 Results

Two sets of data were generated. The first set was the extensometer and applied load readings, while the second set was the grid spacing measurements. Shown in Figure 11 is the stress-strain curve for the 2 inch gauge length specimens.

Figures 12a & b represent the grid extension after testing (plastic strain) versus the fracture location on the specimen. Position 5 is where the specimens fractured. From these graphs, it appears that there was no direct relationship with temperature. However, it became apparent that the magnitudes of the curves were influenced by the position where failure occurred with respect to the grid line. The unsymmetrical points of each curve provided this clue. What is meant by unsymmetrical, is that the relative points on the opposite sides of the individual curves experienced different strains. For example, specimen 5a, from Figure 12a, had a distance of 0.275 mm from the first grid-line to the fracture on the left side of the fractured specimen. The right side of the fractured specimen had a distance of 0.125 mm from the first grid-line to the fracture. The red line on Figure 12a indicates this difference.

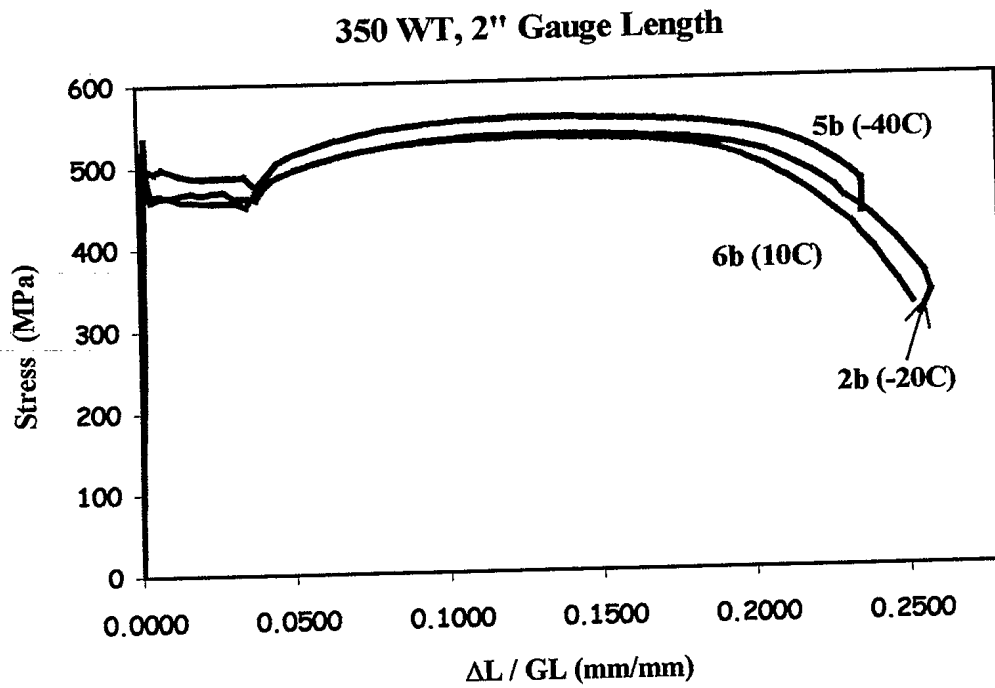


Figure 11. Two Inch Gauge Length Tensile Test Data.

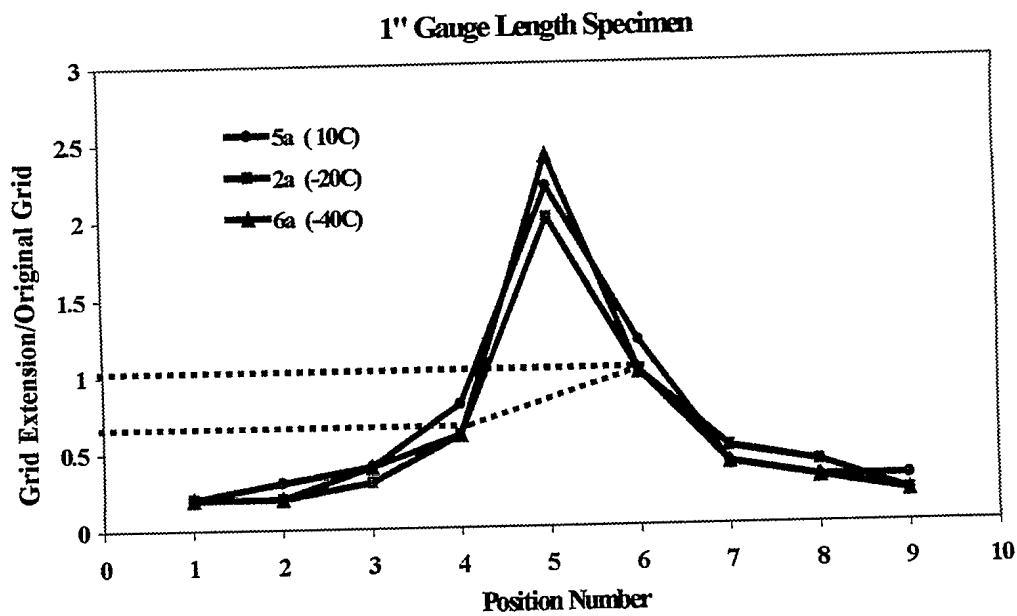
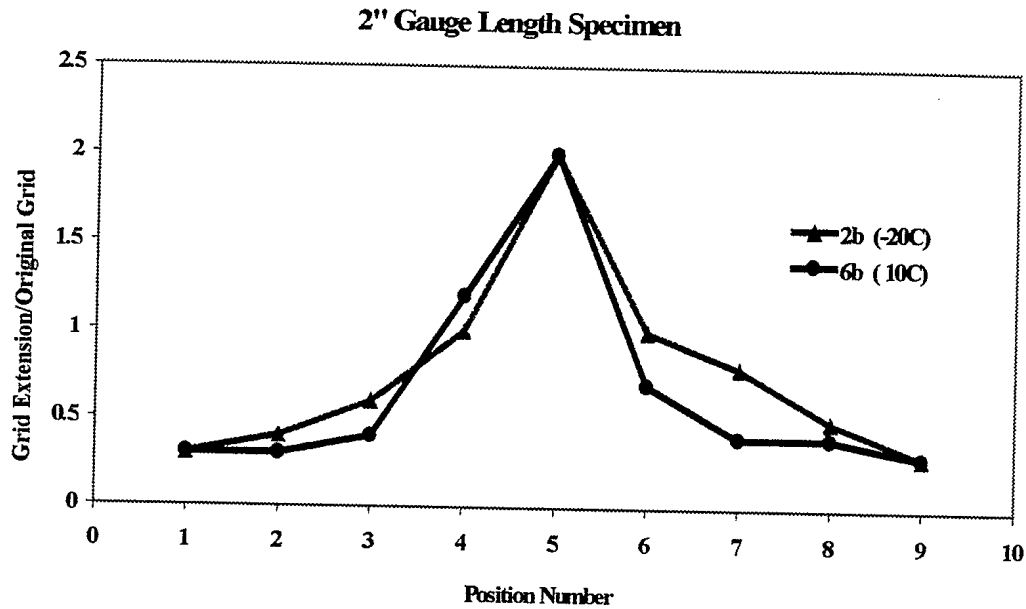


Figure 12a. One Inch Gauge Length Grid Extensions.





**Figure 12b. Two Inch Gauge Length Grid Extensions.**

Figure 13 illustrates the distance from the fracture to the closest grid-line. The thick vertical line represents the location of the fracture. The 1" specimens are identified by the *a* suffix, while the 2" specimens are identified by the *b* suffix. The rectangle represents the distance from the fracture to the grid-line. The best result occurred with specimen 6a, the distance to the nearest grid-line, from the fractured end, on both pieces were very close in length. For example, on side A the grid-line was found to be 0.25 mm from the fracture, while on side B the grid-line was found to be 0.175 mm from the fracture.

Specimen 5a and 2b also had lengths that were fairly similar in their distances from the fractured end to the nearest grid-line. Specimen 6b fractured on the grid-line, it was the only specimen to do so.

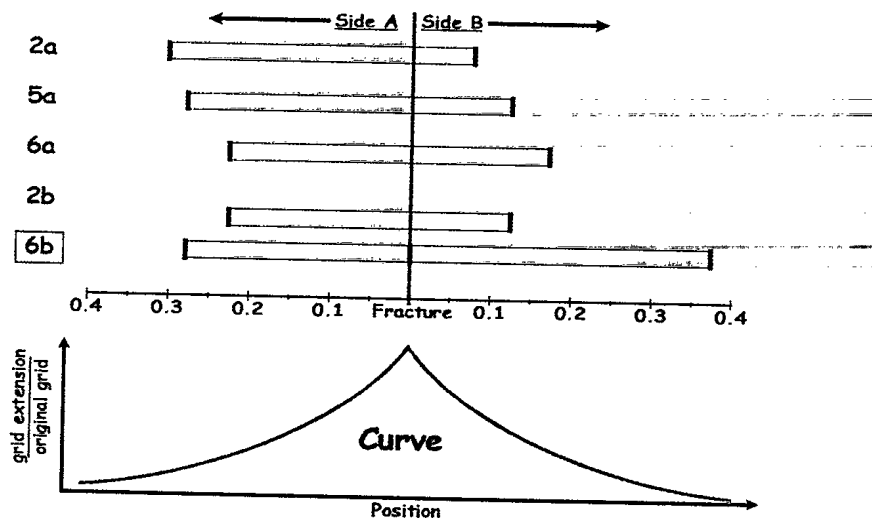


**Figure 13. Fracture Locations.** (a identifies 1" & b identifies 2" specimens)

The five closest grids on both sides of the fractured specimens were measured, and the percent strain calculated. Figure 14a displays the stress versus percent strain for the tested specimens. The areas under these curves are the critical strain energy density for the tested specimens. It is difficult to obtain relevant information from these curves. However, averaging the stress and the percent strain for the 1 and 2 inch specimens at each temperature results in the graph shown Figure 14b. It is apparent from this graph that there is a direct relationship with temperature. The area under the curve for the specimen tested at  $-40^{\circ}\text{C}$  was approximately 53000, the area under the curve for the specimens tested at  $-20^{\circ}\text{C}$  was approximately 61000, and the area under the curve for the specimens tested at  $10^{\circ}\text{C}$  was approximately 64000. As the temperature increased so did the area under the curves.

Real Stress- Real Strain Curves for 1.125 cm Gauge Length

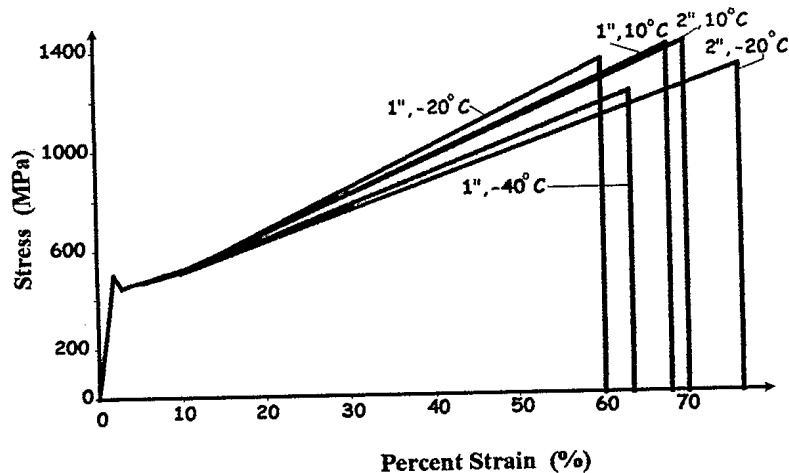


Figure 14a. Real Stress - Real Strain Curves for 1.125 cm Gauge Lengths.

Real Stress- Real Strain Curves for 1.125 cm Gauge Length

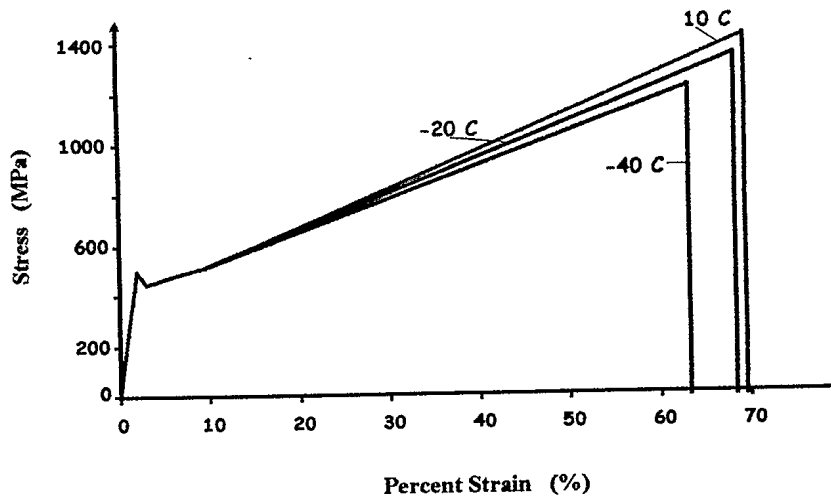


Figure 14b. Averaged Real Stress - Real Strain Curves for 1.125 cm Gauge Lengths.

## 8.0 Conclusions

In this study the focus was on critical strain energy density and strain to fracture for the transition zone. In the transition zone, a direct relationship between the critical strain energy density and the plastic strain over 1.125 cm, was found with temperature.

## 9.0 Recommendations

The real stress - real strain test procedure must be improved to acquire real stress and real strain of at least 10 points along the curve.

The grid should be etched onto all four sides of the specimens. To increase accuracy in determining fracture strain, the grid on one face of the specimen should have an offset to the adjacent face.

Techniques to accurately acquire strain to fracture over smaller and smaller gauge lengths, need to be developed. Ideally, it may be necessary to match the specimen gauge length with finite element mesh size.

## 10.0 References

1. Rolfe S.T., Barsom J.M., Fracture and Fatigue Control In Structure: Applications of Fracture Mechanics, Prentice-Hall, USA 1987, pp. 2.
2. Manchester Material Science Center, [www/umist.ac.uk/MatSc/liberty](http://www.umist.ac.uk/MatSc/liberty).
3. H.C. Campbell, "Brittle Fracture and Structural Failure of the Liberty Ships", 1967.
4. American Bureau of Shipping, "Surveyor", Democrat Press, Vol. 23, No. 2, June 1992, pp.32.
5. Biggs W.D., The Brittle Fracture Of Steel, MacDonald & Evans, Great Britain, 1960.
6. Thomson R. & Champion C.S., "Fracture Toughness Evaluation of Steels for Arctic Marine Use", CANMET, Canada, 1983.
7. Lawn B.R., Wilshaw T.R., Fracture of Brittle Solids, Cambridge University Press, Cambridge, 1975.
8. [Http://ranger.eng.tau.ac.il/history](http://ranger.eng.tau.ac.il/history)
9. Admiralty Ship Welding Committee, "First and Second Interim Reports", Great Britain, 1946 and 1948.

10. J.R. Matthews, J. F. Porter and C.V. Hyatt, "Fracture Control for Submarine Pressure Hulls II", Prepared for the third meeting of the TTCP PTP1 Operating Assignment on Fracture Control of Naval Structures, Annapolis Maryland, May 1-3, 1991.
11. J.R. Matthews, "Ship Fracture", Paper Presented at the 3rd CF/CRAD Meeting on Naval Applications of Material Technology, Halifax, NS. April 22-24, 1997, pp. 409-29.
12. G. E. Dieter, Mechanical Metallurgy, 2<sup>nd</sup> ed., McGraw-Hill, New York, 1976.
13. J. R. Matthews, "Prediction of Ductile Behaviour in Welded Structures (Transition Behaviour, Shear Lip, Notch Acuity and Specimen Size)", The Minerals, Metals & Material Society, 1997.
14. P. Matic, G.C. Kirby III and M.I. Jolles, "The Relationship of Tensile Specimen Size and Geometry Effects to Unique Constitutive Parameters for Ductile Materials", NRL Memorandum Report 5936, Office of Naval Research, Arlington, VA, 1987.